

Characterization of Silicon Nitride Micromechanical Cantilevers and Bridges

Sam Bader

Abstract—Nanoindentation is performed upon micron-thick silicon nitride cantilevers and bridges with in-plane dimensions in the tens of microns. Deflection models for such structures are evaluated and the material is characterized in terms of its Young’s modulus and residual stress. This provides the constants necessary for micromechanical engineering with low pressure chemical vapor deposition silicon-rich silicon nitride layers. Micro-cantilever tests yielded a Young’s Modulus of $E = 198 \pm 14$ GPa, and a micro-bridge test yielded $E = 171 \pm 58$ GPa, which is in the range of previously reported values.

Index Terms—MEMs, Cantilever, Bridge, Silicon Nitride

I. INTRODUCTION

MICROMECHANICAL devices, ranging from the accelerometers in an iPhone to silicon pressure sensors in tires, rely on precisely measured material properties in the same way that their macroscale equivalents do [1], however, their size makes such properties more difficult to evaluate. In general the vital material constants for the mechanical engineering of such devices, the Young’s modulus and the residual stress, are obtained by bending tests [1, 2] under nanoindentation. In this letter, the nanoindentation technique is employed upon micro-cantilevers and micro-bridges to characterize a thin film of Low Pressure Chemical Vapor Deposition (LPCVD) silicon-rich silicon nitride and determine the characteristic mechanical values.

II. METHODS

The experiment utilizes two cantilevers, one $50 \times 100 \mu\text{m}$ and one $20 \times 100 \mu\text{m}$ (where the names indicate *width* \times *length*), as well as one $10 \times 50 \mu\text{m}$ bridge (where the name indicates *bridge width* \times *gap width*). See Figure 1 for marked dimensions.

A. Fabrication

The starting material was a silicon wafer with a thin layer of low-stress, silicon-rich silicon nitride deposited by LPCVD. Before device fabrication, the sample was characterized using the KLA Tencor UV1280 Film Thickness Measurement System; the important parameters of the fabrication and characterization which are known to affect the device’s mechanical properties are collected for reference into Table I.

The cantilever and bridge structures were plasma etched in a sulfur hexafluoride chemistry from the top layer of silicon nitride. An anisotropic KOH etch (20% KOH by weight) was performed to undercut the silicon and release the silicon

TABLE I
CONDITIONS FOR LPCVD GROWTH OF THE SAMPLE

Pressure	Temperature	Ratio $\text{SiH}_2\text{Cl}_2:\text{NH}_3$	Final thickness
250mTorr	675°C	10:1	1.2 μm

nitride cantilevers and bridges. The final sample was glued to a magnetic plate for testing.

Optical images of finished devices are shown in Figure 1. The approximately $10 \mu\text{m}$ -wide lighter regions around the borders of all gaps indicate etching of the silicon substrate under the silicon nitride, and furnish an estimate of the extent to which structural supports were undercut in the KOH etch. This effect will be discussed further in the uncertainty analysis.

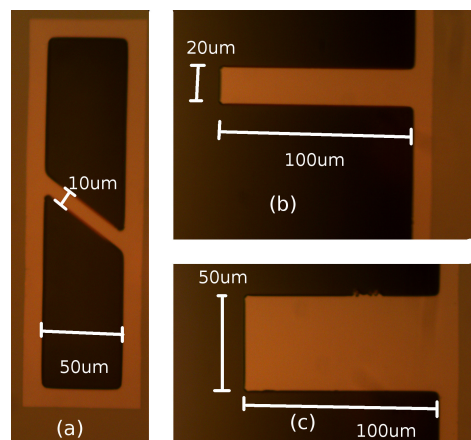


Fig. 1. Optical micrographs of (a) the $10 \times 50 \mu\text{m}$ bridge (b) the $20 \times 100 \mu\text{m}$ cantilever and (c) the $50 \times 100 \mu\text{m}$ cantilever, with dimensions annotated. The cantilevers were measured to have the indicated dimensions to within one micron, and the bridge was measured to be $75 \mu\text{m}$ along the slanted length. Notice the undercutting (lighter regions of the borders) extends about $10 \mu\text{m}$ in from the gap.

B. Testing

These devices were tested with a Hysitron Triboindenter [3] in order to determine the Young’s modulus (E) and, in the case of the bridges, residual stress (σ_0).

Two cantilevers were tested: a $50 \times 100 \mu\text{m}$ and a $20 \times 100 \mu\text{m}$ version, and the force-displacement curves were analyzed to determine Young’s modulus. Although the force-displacement curve $F(x)$ of a cantilever is a function of both load position and Young’s modulus, the undercutting inherent to this fabrication procedure makes the starting location of the cantilever an ill-defined quantity. However, by performing the indentation experiment at multiple locations along the structure as discussed below, the dependence upon absolute

S. Bader is with the Department of Physics, Massachusetts Institute of Technology, Cambridge, MA 02139 USA. Contact: sbader@mit.edu

Manuscript received October 23, 2013.

positioning was reduced to a fitting parameter, so that Young's modulus could be extracted.

Additionally, one force-displacement curve was obtained from the center of a 10x50 μm bridge, and a fit to this curve provided information about both the Young's modulus and residual stress. The features of these curves and their fits are presented alongside the calculation in Sec. III

III. RESULTS AND DISCUSSION

This section will first explain the analysis of the cantilevers, then that of the bridges, and then discuss the results obtained.

A. Cantilever Analysis

As mentioned, each cantilever was indented at three locations. At each location, the indenter was programmed to push three times sequentially with increasing force, as shown in Figure 2(a), in order to generate one linear, elastic force-displacement curve, like that shown in Figure 2(b).

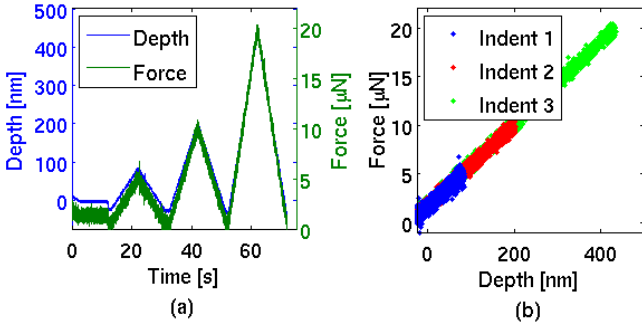


Fig. 2. The force-displacement curve for a 20x100 μm cantilever indented approximately 80 μm from the tip. (a) shows the depth and force measured versus time as three indentations were applied, and (b) graphs the force versus displacement, coloring separately the curves for each indentation. Since the curves in (b) all overlap, this is an elastic (non-hysteretic) process.

For the 20x100 μm cantilever, a curve such as shown in Figure 2(b) was produced at each of three locations: 80, 60, and 40 μm from the tip. All three curves are plotted together in Figure 3. Each curve was fit to within the spread of the data by a linear Hooke's law $F = kx$. In these fits, a constant offset was allowed (ie the fits do not run through the origin) to account for any calibration error.

The same was done for the 50x100 μm cantilever (at locations approximately 60, 40, and 20 μm from the tip). The mechanical theory of small deflections relates the spring constant k of a cantilever with width W and thickness H at a given length L , to the Young's modulus, E via

$$k = \frac{EWH^3}{4L^3}. \quad (1)$$

Thus a plot of $k^{-1/3}$ versus location (as shown in Figure 4) should be linear with a slope $-b$ such that

$$E = 4/wt^3b^3. \quad (2)$$

(Note: the slope is negative, because L in Eq. 1 is defined from the fixed end of the cantilever, whereas, in this procedure, location is approximated from the free end of the cantilever.) These curves for both cantilevers are fitted in Figure 4.

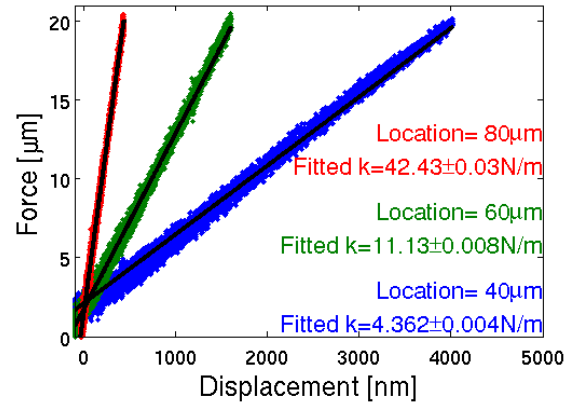


Fig. 3. All three force-displacement curves for the 20x100 μm cantilever, and their fitted spring constants.

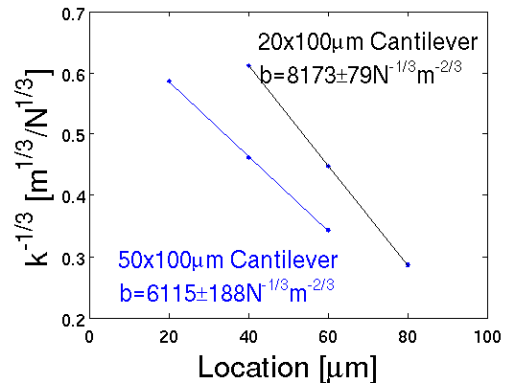


Fig. 4. Variation of the spring constant with location along the cantilever measures the Young's modulus via Eq 2. Note that the point markers are actually small errorbars from the small fitting uncertainties in Figure 3.

Using Eq. 2 and the fitted values for b , one can determine E , with the caveat that the 50x100 μm cantilever is actually more of a plate than a cantilever. This distinction is modelled by replacing its Young's modulus in Eq. 1 by its plate modulus

$$E \rightarrow \frac{E}{1 - \nu^2} \quad (3)$$

where $\nu \approx .3$. In the end, this correction simply means the E drawn from the 50x100 μm cantilever should be multiplied by a factor of $(1 - \nu^2) \approx .91$. Taking this into account, the Young's moduli of the two cantilevers are 212GPa and 184GPa for 20x100 and 50x100 μm respectively. These values are averaged and a final uncertainty is estimated from their spread to conclude that

$$E = 198 \pm 14\text{GPa}$$

B. Bridge Analysis

Similarly, the indenter was programmed to indent multiple times into the center of the bridge, and the resulting curves are shown in Figure 5.

Although the plot shows a hysteresis, it is so small that push and release curves were just averaged together to generate a single force-displacement curve for the 10x50 μm bridge, as shown in Figure 6. The curve is clearly non-linear, so, it will

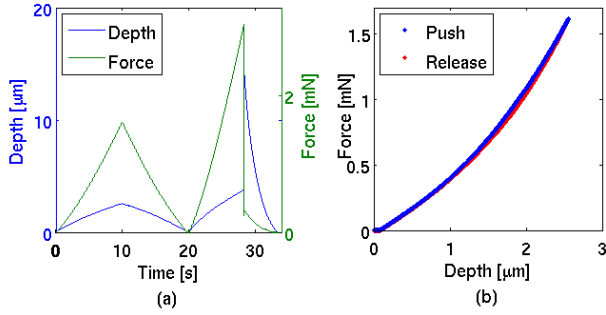


Fig. 5. (a) The measured force-displacement curves for the bridge versus time. Note that the bridge collapsed just before $t = 30$ s, which explains the sudden discontinuities. (b) The force versus displacement curve for only the completed indentation, showing a small hysteresis between the pushing curve and the releasing curve.

be necessary to take the theory of deflections for a bridge to the next non-zero order (third):

$$F = \left\{ \left(\frac{\pi^2}{2} \right) \left(\frac{\sigma_0 W H}{L} \right) + \left(\frac{\pi^4}{6} \right) \left(\frac{E W H^3}{L^3} \right) \right\} x + \left\{ \left(\frac{\pi^4}{8} \right) \left(\frac{E W H}{L^3} \right) \right\} x^3 \quad (4)$$

where W is the width, H is the thickness, L is the length, σ_0 is the residual stress, and E is again the Young's modulus. Note that the length is not actually the $50\mu\text{m}$ of the gap, because the bridge is constructed at a slant of 54.7° , resulting in a measured length of $L = 75\mu\text{m}$, as in Figure 1.

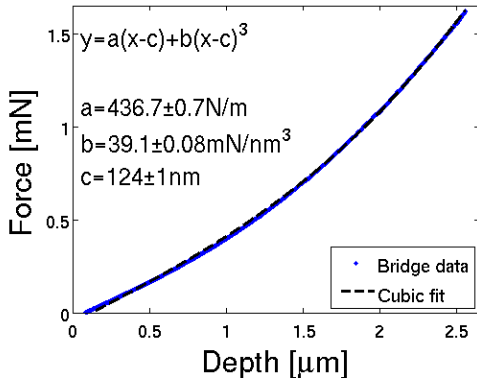


Fig. 6. Averaged force vs displacement curve for the bridge, fit to a cubic polynomial as in Eq. 4. Note, a linear offset is again allowed in the position to account for miscalibration: the curve does not begin at $x = 0$.

The curve is thus fitted as in Figure 6, and from the cubic coefficient, one can use Eq 4 to extract E , and then use that value of E , as well as the linear coefficient, to extract σ_0 . This procedure gives $E = 112.9 \pm .2\text{GPa}$, and $\sigma_0 = 458 \pm 1\text{MPa}$. However, there is one large source of error which must be accounted for beside the fitting uncertainties. Undercutting during the wet etch creates compliant supports for the bridge, which can be modelled as an effective addition to the bridge length. This was not as vital a concern in the case of the cantilever, where the fitting method reduced the length dependence, but it can have a significant impact upon the bridge results because only one point was indented.

To account for this, one can run the same calculation but allowing for $10\mu\text{m}$ (see Figure 1) of undercutting on either side

of the bridge: this brings the total effective length to a generous $L = 95$. Plugging back in to Eq 4 gives $E = 229.4\text{GPa}$, and $\sigma_0 = 580\text{MPa}$. Averaging this estimate with the previous ($L = 75\mu\text{m}$) estimate gives a final value for the parameters of the bridge. Uncertainties are taken from the difference in these two estimates:

$$E = 171 \pm 58\text{GPa}, \quad \sigma_0 = 519 \pm 61\text{MPa}$$

The final results are summarized for reference in Table II.

C. Discussion

The results thus far have been self-consistent, in that the value of Young's modulus measured from the cantilevers and that from the bridge fall within each other's uncertainty. This cantilever approach is shown to yield higher precision parameters than the bridge approach. This is because the uncertainty in the bridge-measured values is dominated by length uncertainty from support undercutting. The cantilever approach is less sensitive to this error source because relative positioning is used and the length error is, to a large extent, absorbed by the offset parameter of the linear fit in Figure 4.

Both measurements of Young's modulus are in the range of previously reported measurements of $E = 156 \pm 20\text{GPa}$ (see [1], Table 1, Specimen A). The residual stress, on the other hand, is about half what would be suggested by [4] (see their Eq. 2), however, all of their experiments were done with lower Si/N ratios (of order 1), which may cause the difference.

TABLE II
FINAL PARAMETER ESTIMATES FROM THE TWO METHODS

Method	E [GPa]	σ_0 [MPa]
Cantilevers	198 ± 14	
Bridge	171 ± 58	519 ± 61

IV. CONCLUSION

This experiment has shown that micromechanical cantilevers do obey a Hooke's law for small displacement, and micromechanical bridges are well-described as non-linear (cubic) springs with mild hysteresis. Quantifying these observations, these tests found values of the Young's modulus for silicon-rich silicon nitride which agree with previously reported values, and have found a value for the residual stress under specific deposition conditions. This provides the fundamental values necessary for micromechanical engineering with silicon nitride layers.

REFERENCES

- [1] G. J. McShane, M. Boutchich, A. S. Phani, D. F. Moore, and T. J. Lu, *J. Micromech. Microeng.*, vol. 16, no. 10, p. 1926, 2006.
- [2] J. Mencika and E. Quandt, *J. Mat. Research*, vol. 14, pp. 2152–2161, 05 May 1999.
- [3] *Ti 900 Triboindenter*, Hysitron. [Online]. Available: <http://www.hysitron.com/products/ti-series/ti-900-triboindenter>.
- [4] P. Temple-Boyer, C. Rossi, E. Saint-Etienne, and E. Scheid, *J. Vac. Sci. Tech. A*, vol. 16, no. 4, pp. 2003–2007, 1998.